Preparation and Study of Regenerated Aerogels and Films from Corncob Cellulose

Xingya Kang,[a] Baoying Wang,[a] Yan Zhang,[a] Yong Huang,[b] Jinzhu Zhang,[c] An Zhang,[c] and Min Wu [b,*]

Corncob cellulose from residue of saccharified agricultural waste corncob was used as a new resource of cellulose to dissolve in 1-allyl-3-methylimidazolium chloride (AmimCl) and then to regenerate in three different coagulation baths: water, 60 wt% AmimCl aqueous solution, and anhydrous ethanol. The effects of the different coagulation baths on the properties of corncob cellulose aerogels and regenerated films were studied. The results showed that the aerogels had porous network structures, and the regenerated films were relatively transparent with high strengths and good thermal stabilities. When 60 wt% AmimCl was used as the coagulation bath, the network of the obtained aerogel was dense and uniform, and the regenerated film had good thermal stability and a tensile strength superior to the films from the other regeneration baths. The films might have uses in packaging or other fields and aid in comprehensive utilization of agricultural wastes.

Keywords: Corncob; Cellulose; Ionic liquid; Regenerate

*Contact information: a: School of Packaging and Printing Engineering, Henan University of Animal Husbandry and Economy, Zhengzhou 450046, People's Republic of China; b: Technical Institute of Physics and Chemistry, Chinese Academy of Sciences, Beijing 100190, People's Republic of China; c: Jinan Shengquan Group Share Holding Co., Ltd., Jinan 250204, People's Republic of China; * Corresponding author: wumin@mail.ipc.ac.cn*

INTRODUCTION

China, as a large agricultural country, produces great quantities of agricultural wastes. Corncob is a relatively common agricultural waste. Generally it has been incinerated, with negative environmental effects. Recently, in the context of sustainable development and environmental protection, the development and utilization of biomass resources, especially agricultural waste, has received increasing attention, and corncob is gradually being developed and utilized (Liu *et al*. 2010; Zhang *et al*. 2010). Saccharification of corncob and extraction of xylose are common development and utilization methods (Procentese *et al*. 2015), but approximately 30% remains as residue. Therefore, this study used the residue of corncob saccharification as a raw material to study its utilization value by dissolution and regeneration.

Ionic liquid (IL), an ionic compound composed of organic cations and inorganic anions, is a large class of green solvents of cellulose. After dissolving, cellulose can be regenerated by adding a non-solvent of cellulose to the solution, namely by employing a coagulation bath. The regeneration process is determined by the inter-diffusion between the solvent and the coagulation bath. Therefore, the composition, concentration, temperature, time, and additives of the coagulation bath will affect the regeneration of the cellulose, which in turn affects the properties of the regenerated hydrogel, aerogel, and film (Sescousse and Budtova 2009; Isobe *et al*. 2011). For cellulose solutions of IL, the common

coagulation baths are water, ethanol, and acetone, which is volatile and has good compatibility with IL (Östlund *et al*. 2013). Among them, water is the most commonly used coagulation bath due to its miscibility with IL and recycling convenience. Recently, Mi *et al*. (2016) used a new coagulation bath, which was a high concentration of IL aqueous solution, to regulate the regeneration process of cellulose to obtain a transparent and flexible cellulose aerogel with high porosity.

In this study, IL was selected as the solvent to study the solubility of corncob cellulose. Then, three different coagulation baths (water, 60 wt% IL aqueous solution, and anhydrous ethanol) were used to study their effects on cellulose regeneration. Finally, the properties of the regenerated corncob cellulose aerogel and film were examined to assess the utilization value of corncob cellulose dissolution and regeneration.

EXPERIMENTAL

Materials

Corncob cellulose was provided by Jinan Shengquan Group Share Holding Co., Ltd. (Jinan, China). Microcrystalline cellulose was purchased from Sigma-Aldrich (St. Louis, MO, USA), and 1-allyl-3-methylimidazolium chloride (AmimCl) was provided by Zhang Jun, researcher of the Institute of Chemistry, Chinese Academy of Sciences (Beijing, China). Anhydrous ethanol and tert-butyl alcohol, analytically pure, were purchased from Beijing Chemical Works (Beijing, China).

Dissolution of Corncob Cellulose

A 2 wt% corncob cellulose solution in AmimCl was prepared by mechanical stirring at 80 °C for 2 h to obtain a transparent solution. Then, the transparent solution was cooled to room temperature, and air bubbles were removed by standing still.

Regeneration of Corncob Cellulose

The corncob cellulose solution was poured onto a clean glass plate and scraped by a four-sided preparation machine with a fixed thickness, and then the plate was immersed into the coagulation bath to regenerate and gel at room temperature. After gelation, the hydrogels were washed several times by using the same solvent with the coagulation bath until no chloride ions were detected by $AgNO_3$.

Preparation of Regenerated Corncob Cellulose Aerogel and Film

The water in the cleaned hydrogel was replaced with tert-butanol to obtain a cellulose tert-butanol gel, which was frozen in liquid nitrogen and then placed on a lyophilizer (FDU-2110, Eyela, Tokyo, Japan) to prepare the corncob cellulose aerogel by freeze drying. The regenerated films were obtained by fixing the cleaned hydrogel on the glass plate and drying at room temperature overnight. The samples obtained from water, 60 wt% AmimCl aqueous solution, and anhydrous ethanol were named Re-W, Re-IL, and Re-E, respectively. The preparation process is shown in Fig. 1.

Characterization

The Fourier-transform infrared (FTIR) spectra were scanned by an FTIR spectrometer (Varian 3100, Palo Alto, CA, USA) in transmission mode in the range of 400 cm^{-1} to 4000 cm^{-1} with a resolution of 2 cm^{-1} and accumulation of 32 scans. The samples

were ground with KBr in a weight ratio of 1:100.

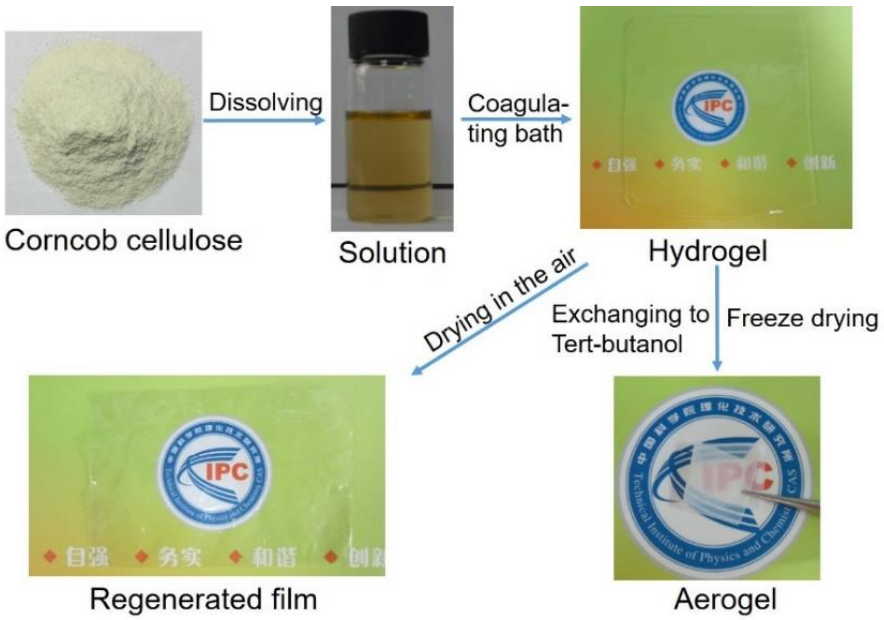

Fig. 1. Preparation processes of regenerated corncob cellulose aerogel and film

X-ray diffraction (XRD) was measured with an X'Pert PRO X-ray diffractometer (Bruker AXS GmbH, Karlsruhe, Germany). The scanning range was from 5° to 60°, and the scanning speed was 2.4°/min, with λ = 0.154184 nm.

Nitrogen adsorption and desorption isotherms were measured by a Quadrasorb SI-MP system (Quantachrome, Boynton Beach, FL, USA). The pore volume and pore size distributions were measured according to the Barrett-Joyner-Halenda (BJH) method. The density of the aerogel (ρ_a) was calculated by dividing its weight by its volume. The porosity of the aerogel (P) was calculated by Eq. 1, where ρ_c was the density of bulk cellulose (1.528 g/cm^3).

$$P\ (\%) = \left(1 - \frac{\rho_a}{\rho_c}\right) \times 100 \quad (1)$$

The surface and cross-sectional morphologies of the aerogels and films were observed using a scanning electron microscope (SEM, Hitachi S-4800, Tokyo, Japan). The cross-sections were first cryofractured in liquid nitrogen.

The mechanical properties of the regenerated films were tested using a universal testing machine (MTS Sintech-1, Eden Prairie, MN, USA). The samples were cut into 5-mm-wide and 30-mm-long strips for tensile testing. The gauge of the strips was 20 mm, and the strain rate was 4 mm/min. The samples were conditioned in a desiccator at 20 °C ± 5 °C for 48 h before testing. Measurements were made for more than five test pieces.

Thermogravimetry of the regenerated films was performed by a thermogravimetric analyzer (Q 50, TA Instruments, New Castle, DE, USA) in nitrogen atmosphere from room temperature to 600 °C with a heating rate of 10 °C/min.

RESULTS AND DISCUSSION

Morphologies of Aerogels

The coagulation bath affects the regeneration and gelation of the cellulose, which affects the intertwining of cellulose molecules during the regeneration process, resulting in different internal structures.

Figure 2 shows the surface morphologies of the aerogels. The 20 K magnification SEM images showed that the surface of aerogel Re-IL was relatively dense, and almost no network was visible. Meanwhile, aerogels Re-W and Re-E displayed clear network structures. The 70 K magnification SEM images showed that aerogel Re-IL had a compact network, while those of Aerogel Re-E and Re-W were loose. Aerogel Re-E's surface was more uniform than that of aerogel Re-W, and the pores were larger.

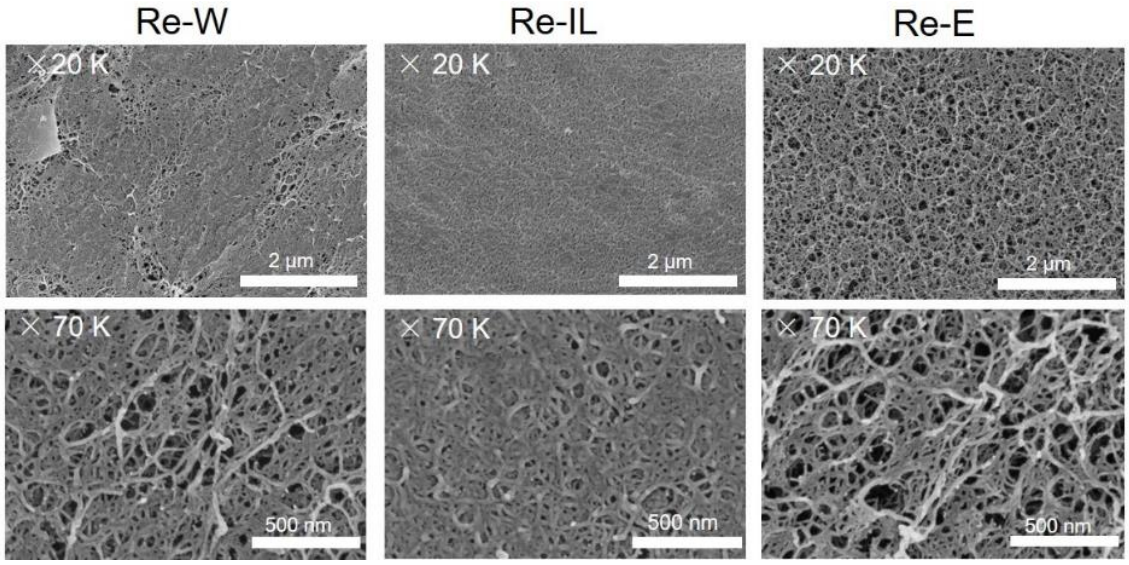

Fig. 2. Surface morphologies of aerogels

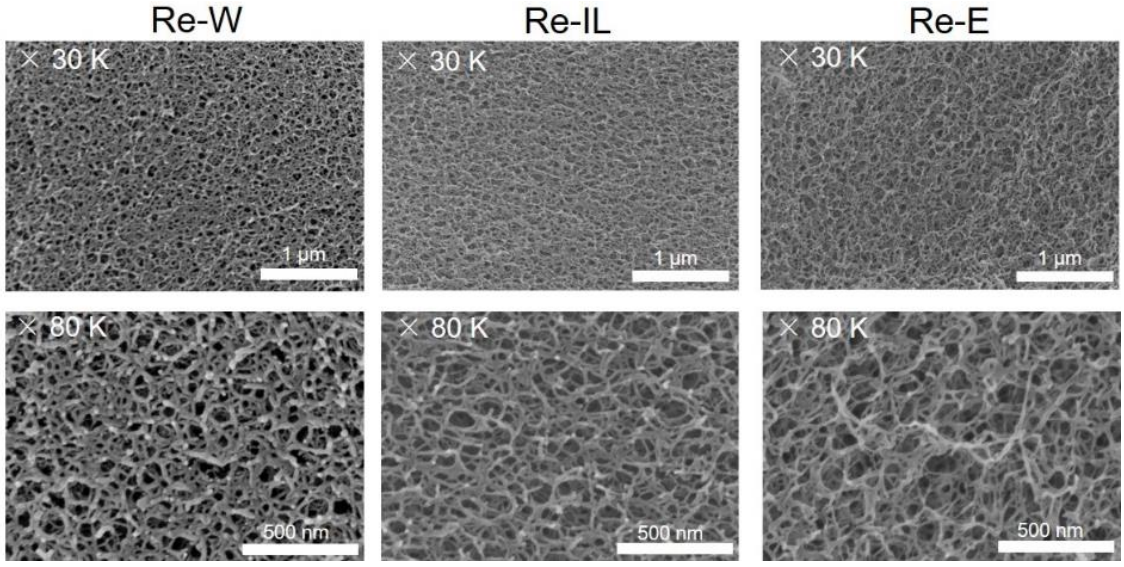

Fig. 3. Cross-sectional morphologies of aerogels

Figure 3 shows the cross-sectional morphologies of the aerogels. The 30 K magnification SEM images indicated that the cross-sections of the aerogels all had clear network structures. The 80 K magnification SEM images indicated that those of aerogels Re-IL and Re-E were relatively uniform, but that of aerogel Re-W was not uniform. This result was related to the speed of regeneration and gelation.

When water was used as the coagulation bath, the regeneration process and entanglement of the cellulose molecular chains were fast, encouraging the formation of a dense network structure. However, when the speed was too fast, a non-uniform network structure was obtained. The water content in 60 wt% AmimCl was low, so the regeneration rate was regulated, making the regeneration and entanglement of the cellulose molecular chains relatively uniform.

When the non-aqueous solvent ethanol was used as the coagulation bath, the compatibility and diffusion speed between ethanol and AmimCl were low. Therefore, the regeneration speed was decreased, and there was sufficient time for the cellulose molecular chains to regenerate and entangle, resulting in a loose and uniform network structure (Hauru *et al*. 2016; Meenatchi *et al*. 2017).

Specific Surface Areas and Pore Size Distributions of Aerogels

The density and porosity of an aerogel can also reflect the compactness of its structure. As shown in Table 1, the specific surface areas of the three aerogels ranged from 226 m^2/g to 270 m^2/g, indicating that the three aerogels were of porous structure. The density of aerogel Re-E was the lowest (0.035 g/cm^3), and its porosity was the greatest (97.8%), further indicating that the aerogel structure obtained from the anhydrous ethanol was the loosest. Those of Re-W and Re-IL were more compact.

Table 1. Physical Properties of Regenerated Cellulose Aerogels Obtained from Different Coagulation Baths

Sample	Density (g/cm^3)	Porosity (%)	S_{BET} (m^2/g)	Pore Volume (cm^3/g)	Pore Size (nm)
Re-W	0.096	94.0	270	1.28	19.0
Re-IL	0.091	94.3	269	1.03	15.3
Re-E	0.035	97.8	226	0.74	13.0

S_{BET} – Brunauer-Emmett-Teller surface area

The nitrogen adsorption and desorption curves of the aerogels (Fig. 4(a) to 4(c)) were type IV with sharp capillary condensation at high relative pressures and obvious hysteresis loops, indicating that the aerogels were of mesoporous structure (Ma *et al*. 2014; Mi *et al*. 2016). Figure 4(d) shows most of the pore sizes were in the range of 3 nm to 100 nm, and the average pore sizes was in the range of 10 nm to 20 nm and pore volumes was up to 1.3 cm^3/g. (Table 1).

FTIR Spectra of Regenerated Films

The FTIR spectra of the regenerated films (Fig. 5) showed no new peaks, indicating that the corncob cellulose was directly dissolved in the AmimCl with no derivatization reaction. After dissolution and regeneration, the hydroxyl stretching vibration peak of cellulose at 3329 cm^{-1} was blue-shifted to 3359 cm^{-1}, indicating that the hydrogen bonding interactions among the cellulose were weakened after regeneration (Cai *et al*. 2008). After regeneration, the vibration peak at 1430 cm^{-1}, which was related to the crystal form of

cellulose I, was weakened; and the vibration peak at 898 cm^{-1}, which was related to the amorphous region, was enhanced, indicating that the crystal form of the corncob cellulose was changed after regeneration (Zhang *et al*. 2005; Yan and Gao 2008).

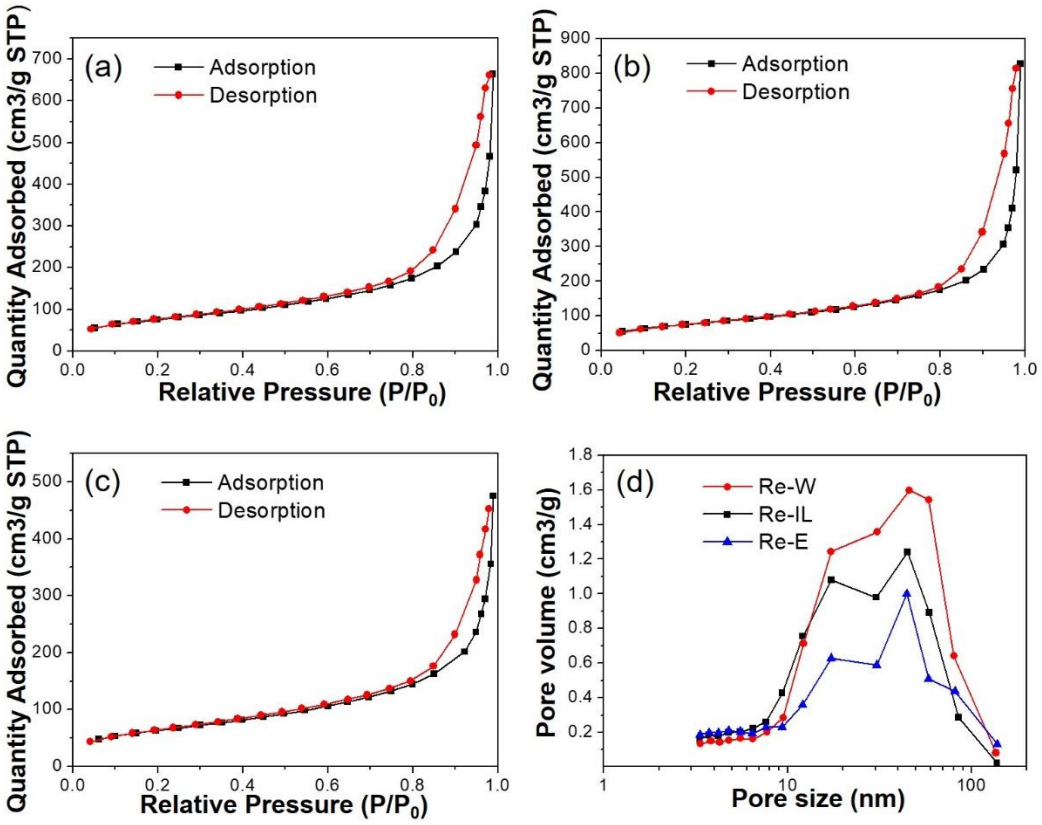

Fig. 4. Nitrogen adsorption and desorption isotherms of (a) Re-W, (b) Re-IL, and (c) Re-E; (d) pore size distribution

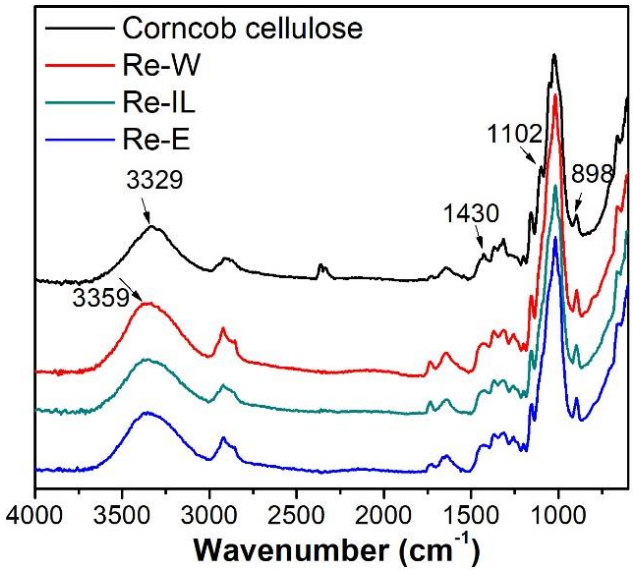

Fig. 5. FTIR spectra of the regenerated films

Crystallinities of Regenerated Films

Generally, after dissolving, the crystal structure of cellulose I disappeared, becoming amorphous. Then, during the regeneration process, the cellulose molecular chains rearranged to form (1-10) crystal planes by hydrophobic interaction (Yamane *et al.* 2006), and then form cellulose II. As shown in Fig. 6, the crystal form of the corncob cellulose was typically cellulose I, which had diffraction peaks at 15.4° and 22.3°. Meanwhile, a broad diffraction peak appeared at approximately 20.7° in the regenerated films, corresponding to the amorphous regions of cellulose. The peak near 12.2° was weak; this was the typical peak of cellulose II. Therefore, after dissolving and regenerating, the crystal form of the corncob cellulose changed from cellulose I to cellulose II, but the degree of crystallinity decreased (Cao *et al*. 2010).

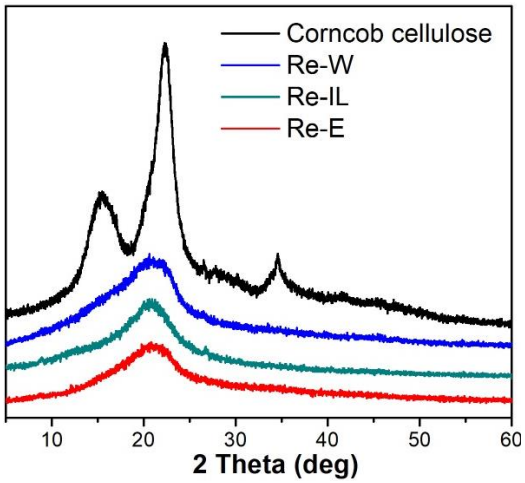

Fig. 6. XRD spectra of regenerated films

Morphologies of Regenerated Films

The corncob cellulose regenerated films were all optically transparent, as shown in Fig. 7. The surface and cross-sectional morphologies of the corncob cellulose regenerated films were all relatively dense and uniform, with no apparent network structure (Figs. 7 and 8), ensuring good mechanical properties of the films.

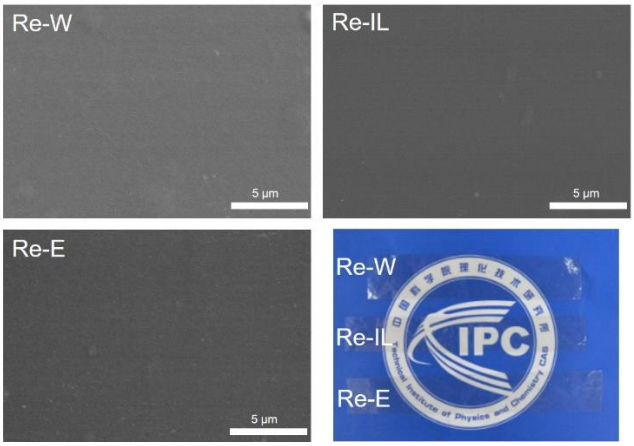

Fig. 7. Surface morphologies and photo of regenerated films

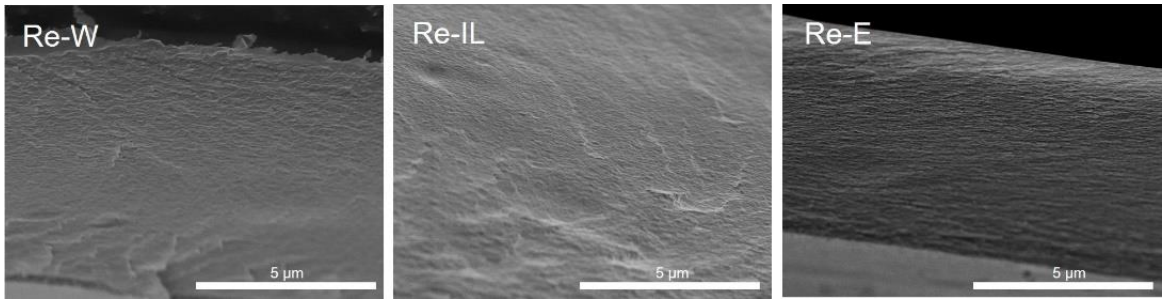

Fig. 8. Cross-sectional morphologies of regenerated films

Mechanical Properties of Regenerated Films

Figure 9 shows the mechanical properties of the corncob cellulose regenerated films. The tensile strengths of films Re-IL, Re-W, and Re-E were 96.87 MPa, 84.43 MPa, and 66.54 MPa, respectively, indicating corncob cellulose regenerated films' good application prospects. During the drying process, as the solvent evaporated, the cellulose molecular chains gradually aggregated and closely aligned. Ethanol evaporated fast, so there was no enough time for cellulose chains aggregated and closely aligned, leading to poor mechanical property of film Re-W. While IL evaporated slowly, so film Re-IL showed strong mechanical property.

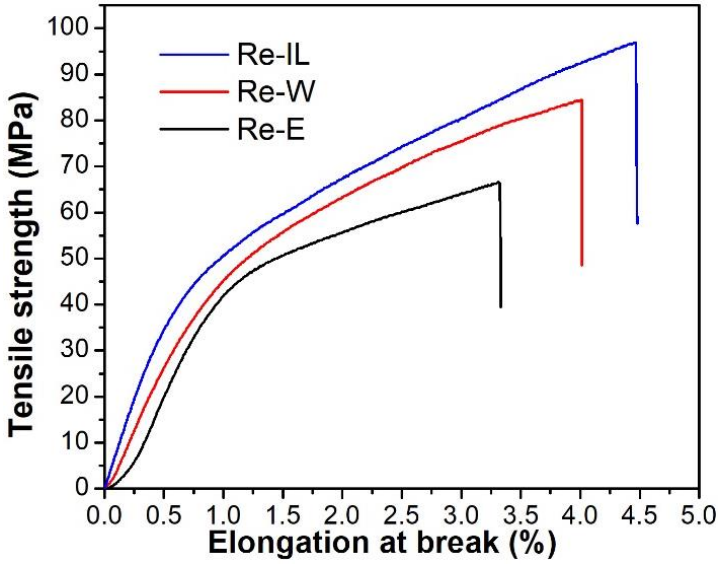

Fig. 9. Mechanical properties of regenerated films

Thermal Stabilities of Regenerated Films

As shown in Fig. 10, the thermal decomposition temperature of the corncob cellulose was 305 °C, and the greatest decomposition rate temperature was 362 °C. Compared with the raw materials, the decomposition temperatures and the decomposition rates of the regenerated films were not greatly reduced; this result was related to the high DP (DP = 940) of the regenerated corncob cellulose. The high decomposition temperatures and greatest decomposition rate temperatures of the regenerated films illustrated their high thermal stabilities.

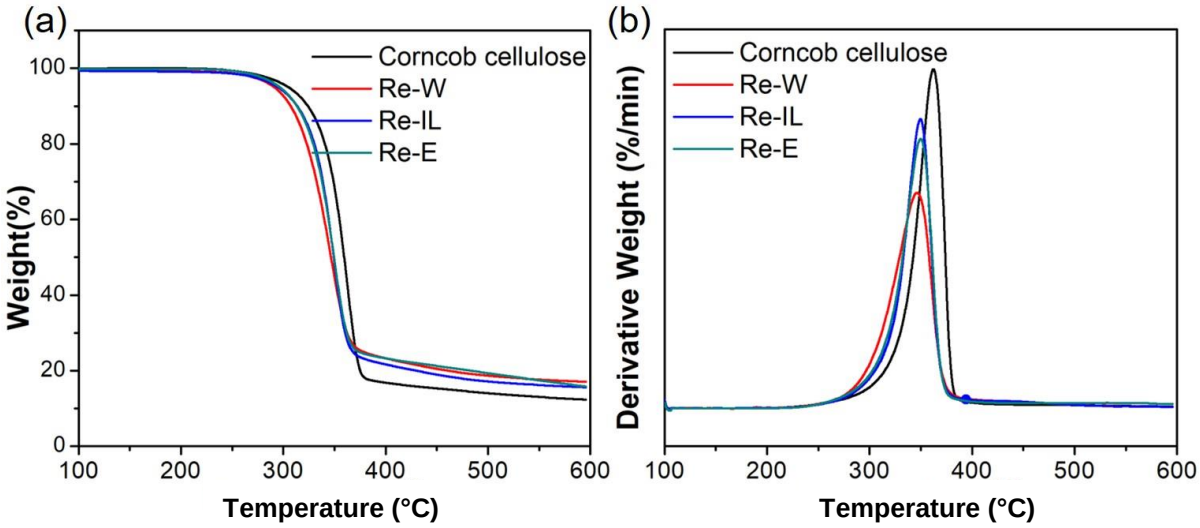

Fig. 10. Thermal degradation of regenerated films under nitrogen: (a) thermogravimetry, (b) derivative thermogravimetry

CONCLUSIONS

1. The residue of saccharified agricultural waste corncob was used as a new resource of cellulose to dissolve in AmimCl and then regenerate to obtain aerogel and film with good performance and mechanical properties, thereby expanding the sources of cellulose raw material and achieving the reuse and added value of agricultural waste.
2. The aerogels were of porous structure and had high specific surface areas, high porosities, and low densities. These properties could be used in many applications, such as adsorption and templates to synthesize nanoparticles. The aerogels obtained from different coagulation baths showed different structures. The aerogel obtained from 60 wt% AmimCl was dense and uniform, the aerogel obtained from water was not uniform, and the aerogel obtained from ethanol was uniform but loose.
3. The regenerated films obtained from different coagulation baths were all transparent and had good mechanical properties and thermal stabilities. When 60 wt% AmimCl was used as the coagulation bath, the obtained regenerated film had the best mechanical properties, and the tensile strength reached 96.87 MPa. Consequently, corncob cellulose films were expected to have uses as packaging materials.

ACKNOWLEDGMENTS

The authors are grateful for the support of the Doctoral Research Initiation Fund of Henan University of Animal Husbandry and Economy, Grant No. 53000179, and College-level key cultivation discipline "Functional Composite Packaging Materials" of Henan University of Animal Husbandry and Economy, Grant No. 503/14020813.

REFERENCES CITED

Cai, J., Zhang, L., Liu, S., Liu, Y., Xu, X., Chen, X., Chu, B., Guo, X., Xu, J., Cheng, H., *et al*. (2008). "Dynamic self-assembly induced rapid dissolution of cellulose at low temperatures," *Macromolecules* 41(23), 9345-9351. DOI: 10.1021/ma801110g

Cao, Y., Li, H., Zhang, Y., Zhang, J., and He, J. (2010). "Structure and properties of novel regenerated cellulose films prepared from cornhusk cellulose in room temperature ionic liquids," *Journal of Applied Polymer Science* 116(1), 547-554. DOI: 10.1002/app.31273

Hauru, L. K. J., Hummel, M., Nieminen, K., Michud, A., and Sixta, H. (2016). "Cellulose regeneration and spinnability from ionic liquids," *Soft Matter* 12(5), 1487-1495. DOI: 10.1039/c5sm02618k

Isobe, N., Kim, U.-J., Kimura, S., Wada, M., and Kuga, S. (2011). "Internal surface polarity of regenerated cellulose gel depends on the species used as coagulant," *Journal of Colloid and Interface Science* 359(1), 194-201. DOI: 10.1016/j.jcis.2011.03.038

Liu, K., Lin, X., Yue, J., Li, X., Fang, X., Zhu, M., Lin, J., Qu, Y., and Xiao, L. (2010). "High concentration ethanol production from corncob residues by fed-batch strategy," *Bioresource Technology* 101(13), 4952-4958. DOI: 10.1016/j.biortech.2009.11.013

Ma, X.-m., Gan, L.-h., Liu, M.-x., Tripathi, P., Zhao, Y.-h., Xu, Z.-j., Zhu, D.-z., and Chen, L.-w. (2014). "Mesoporous size controllable carbon microspheres and their electrochemical performances for supercapacitor electrodes," *Journal of Materials Chemistry A* 2(22), 8407-8415. DOI: 10.1039/c4ta00333k

Meenatchi, B., Renuga, V, and Manikandan, A. (2017). "Cellulose dissolution and regeneration using various imidazolium based protic ionic liquids," *Journal of Molecular Liquids* 238, 582-588. DOI: 10.1016/j.molliq.2016.05.008

Mi, Q.-y., Ma, S.-r., Yu, J., He, J.-s., and Zhang, J. (2016). "Flexible and transparent cellulose aerogels with uniform nanoporous structure by a controlled regeneration process," *ACS Sustainable Chemistry & Engineering* 4(3), 656-660. DOI: 10.1021/acssuschemeng.5b01079

Östlund, Å., Idström, A., Olsson, C., Larsson, P. T., and Nordstierna, L. (2013). "Modification of crystallinity and pore size distribution in coagulated cellulose films," *Cellulose* 20(4), 1657-1667. DOI: 10.1007/s10570-013-9982-7

Procentese, A., Johnson, E., Orr, V., Campanile, A. G., Wood, J. A., Marzocchella, A., and Rehmann, L. (2015). "Deep eutectic solvent pretreatment and subsequent saccharification of corncob," *Bioresource Technology* 192, 31-36. DOI: 10.1016/j.biortech.2015.05.053

Sescousse, R., and Budtova, T. (2009). "Influence of processing parameters on regeneration kinetics and morphology of porous cellulose from cellulose–NaOH–water solutions," *Cellulose* 16(3), 417-426. DOI: 10.1007/s10570-009-9287-z

Yamane, C., Aoyagi, T., Ago, M., Sato, K., Okajima, K., and Takahashi, T. (2006). "Two different surface properties of regenerated cellulose due to structural anisotropy," *Polymer Journal* 38(8), 819-826. DOI: 10.1295/polymj.PJ2005187

Yan, L., and Gao, Z. (2008). "Dissolving of cellulose in PEG/NaOH aqueous solution," *Cellulose* 15(6), 789-796. DOI: 10.1007/s10570-008-9233-5

Zhang, H., Wu, J., Zhang, J., and He, J. (2005). "1-allyl-3-methylimidazolium chloride room temperature ionic liquid: A new and powerful nonderivatizing solvent for cellulose," *Macromolecules* 38(20), 8272-8277. DOI: 10.1021/ma0505676

Zhang, M., Wang, F., Su, R., Qi, W., and He, Z. (2010). "Ethanol production from high dry matter corncob using fed-batch simultaneous saccharification and fermentation after combined pretreatment," *Bioresource Technology* 101(13), 4959-4964. DOI: 10.1016/j.biortech.2009.11.010

Article submitted: June 24, 2019; Peer review completed: August 25, 2019; Revised version received: September 3, 2019; Accepted: September 4, 2019; Published: September 9, 2019.
DOI: 10.15376/biores.14.4.8413-8423